CrystEngComm

Accepted Manuscript

Journal Name

COMMUNICATION

Supramolecular ordering of difuryldiketopyrrolopyrrole: the effect of alkyl chains and inter-ring twisting

Chaoying Fu,[a] Francine Bélanger-Gariépy [b] and Dmitrii F. Perepichka*[a]

We report the first study of supramolecular ordering of difuryldiketopyrrolopyrrole (DFDPP), an important building block for semiconducting materials, in 3D crystals and 2D monolayer films. A combined X-ray diffraction (XRD), scanning tunnelling microscopy (STM) and density functional theory (DFT) calculations underlie the mutual roles of alkyl chains and pending aryl substituents on molecular planarity and packing.

Diketopyrrolopyrrole (DPP) derivatives, originally developed as high performance industrial pigments,[1] have recently emerged as some of the most promising semiconducting materials in various optoelectronic applications including organic field-effect transistors (OFETs), photovoltaics (OPVs) and light-emitting diodes.[2,3,4,5] Rigid non-aromatic structure and strong electron deficiency of DPP unit, makes it an ideal building block for low band polymers, when conjugated with various electron-rich (hetero)aromatic substituents. [6] Accordingly, many donor-acceptor DPP copolymers show record high field-effect mobility and photovoltaic efficiency.[7] Significant effort has already been made in structural optimization of DPP-based materials towards enhancing their charge transport properties. Several studies have looked in the role of aromatic co-monomers and alkyl side chains on the planarity of the DPP copolymer backbone and crystallinity of thin films thereof, both of which affect the charge transport in devices.[3,6]

Among the many donor-acceptor DPP-based materials, furan substituted DPP is of particular interest. Furan-based materials are biodegradable and can be generated from renewable sources. Lower aromaticity and higher rigidity of oligo-/polyfurans leads to increased conjugation comparing the thiophene (or phenylene) based structures.[8] In addition, smaller size of oxygen vs sulfur can lead to denser packing/more efficient π-orbital overlap which is important for efficient charge transport in devices.[9,10] Since the first introduction of furan into the DPP-based polymers by Fréchet and coworkers,[11] a number of furan/DPP copolymers and large oligomers have been studied in a quest for yet more efficient materials for OFET, OPV and related devices.[12,13,14,15,16,17,18] The role of furan vs other aromatic linkers in dictating the planarity, crystallinity and π-stacking is discussed in many of these papers, but the conclusions are at times contradictory, and the exact cause-effect relationships are not easy to establish in such complex polymeric systems.

In this communication, we study the supramolecular assembly of small model furan/DPP molecules (DFDPP-C_6 and DFDPP-C_{14}) in 2D monolayer films, by STM, and single crystals (3D),‡ by XRD analysis. Comparing their molecular and supramolecular structure with that of thienyl (DTDPP-C_6) and phenyl (DPDPP-C_6) substituted analogues, we shed light on the effects of the heteroaromatic ring and alkyl chains on the planarity and supramolecular packing of DPP-based materials.

DFDPP-C_6 (R = hexyl)
DFDPP-C_{14} (R = tetradecyl)

DTDPP-C_6

DPDPP-C_6
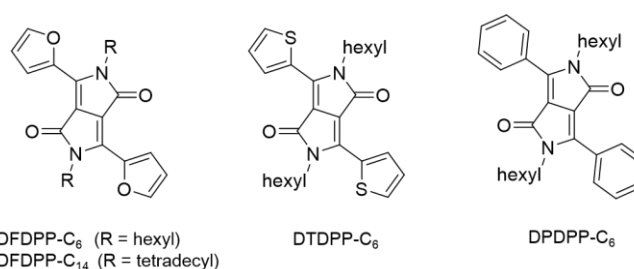
Both DFDPP show a highly planar structure in the crystals, which contrast a slightly (10°) or significantly (35°) increased interring twist in DTDPP[19] and DPDPP.[20] In addition, the planar conformation of DFDPP leads to a tighter π-π stacking: the interplanar distance in DFDPP-C_6 (3.32 Å) is much shorter than that in DPDPP-C_6 (4.11 Å)[20] and DTDPP-C_6 (3.50 Å)[19] (Table 1). This is expected to result in similar or ever higher charge mobility in DFDPP derivatives comparing to their thiophene counterparts, as suggested earlier for other oligofurans.[9,10,21] The even shorter interplanar contacts in DFDPP-C_{14} (3.30 Å) can be attributed to the "compressing" effect of the longer alkyl chains observed for other semiconductors.[22] In all cases, the alkyl chains are oriented nearly orthogonal to theDPP plane.

[a.] Department of Chemistry and Center for Self-Assembled Chemical Structures, McGill University, 801 Sherbrooke Street West, Montréal, Quebec, Canada H3A 0B8. Email: dmitrii.perepichka@mcgill.ca

[b.] Departement de Chimie, Université de Montréal, Montréal, QC, Canada, H3T 1J4.

Journal Name

COMMUNICATION

Table 1 Structural characteristics of DFDPP-Cn single crystals and the other two dialkylated DPP derivatives.

Compound	DFDPP-C$_{14}$	DFDPP-C$_6$	DTDPP-C$_6$ [19]	DPDPP-C$_6$ [20]
a (Å)	18.8248(10)	28.9402(9)	14.682(4)	13.4809(11)
b (Å)	4.6921(3)	4.8707(2)	5.3913(13)	5.5393(3)
c (Å)	21.4035(11)	17.3118(6)	15.704(4)	17.4838(14)
β (°)	100.903(3)	107.785(2)	97.355(4)	90.218(7)
Z	2	4	2	2
H...O=C length (Å)	-	2.434	2.712	2.429
H… O=C angle (°)	-	162.36	122.06	149.64
Ar/DPP torsion (°)	3.97	0.86	10.04	34.88
C-C-N-C torsion (°)	88.44	95.86	89.71	78.22
interplanar distance (Å)	3.30	3.32	3.50	4.11
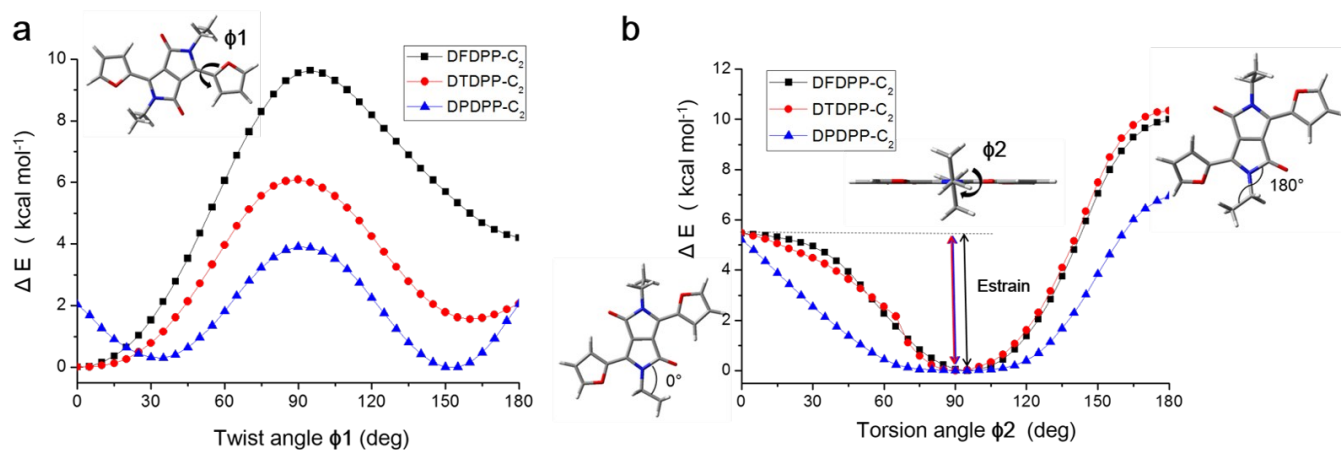
Fig. 1 Gas-phase calculated (a) interring twisting potentials and (b) C-C-N-C bond torsion energies of DFDPP-C2, DTDPP-C2 and DPDPP-C2 (M06-2X/6-31G(d)).

The effect of the aryl groups on the molecular structure of DPP derivatives was further examined by DFT calculations at the M06-2X/6-31G(d) level. Nearly planar conformations for DFDPP ($\phi1$ = 2.0°) and DTDPP ($\phi1$ = 2.4°) and a substantial interring twist for DPDPP ($\phi1$ = 31.3°) are predicted in the gas phase, in agreement with the single crystal XRD analysis. Figure 1 shows the potential energy of the relaxed molecules with one constrained coordinate: the dihedral angle $\phi1$ or $\phi2$, for the interring and alkyl chain out-of-plane twist, respectively. The calculated interring twisting potentials (Fig. 1a) also indicate that DFDPP is much more rigid than DTDPP, which explains the slightly larger twisting angle of DTDPP observed in single crystals (Table 1). It was earlier suggested, based on DFT calculations, that intramolecular S…O contacts are responsible for planarization of DTDPP moiety.[6] Our results (Fig. 1a), however, show that such interaction (occurring at $\phi1$

~160°) is less favourable than an alternative H…O interaction ($\phi1$ = 0°) by ca. 1.5 kcal/mol per thiophene ring.

Comparing the two DFDPP crystal structures (Fig. 2 and 3) shows that varying the alkyl chain length on DFDPP slightly changes the packing arrangement (DFDPP-C$_{14}$: space group P2$_1$/c with two non-equivalent molecules per unit cell; DFDPP-C$_6$: space group C2/c with four non-equivalent molecules per unit cell). However, the key intermolecular interactions remain the same: in both cases the DFDPP cores form π-stacks along the *b* axis, and are separated by interdigitated alkyl chains along the *a* axis (Figs. 2,3a). The only material difference is that the (nearly orthogonal) molecules in adjacent π-stacks (along axis c) contact each other via either edge-to-face CH-π interactions of furan rings (DFPDPP-C$_{14}$, Fig. 2b) or a weak H-bonding between DPP oxygen and β-furyl hydrogen (DFPDPP-C$_6$, Fig. 3b). Similar close contacts were also observed in the

Journal Name

COMMUNICATION

DTDPP-C_6 and DPDPP-C_6, but DFDPP-$2C_6$ experiences the strongest H bonding among the three derivatives (judged by shorter H…O=C distance and a more favorable H bonding angle, Table 1), likely attributable to the more polarized CH bond in the furan.
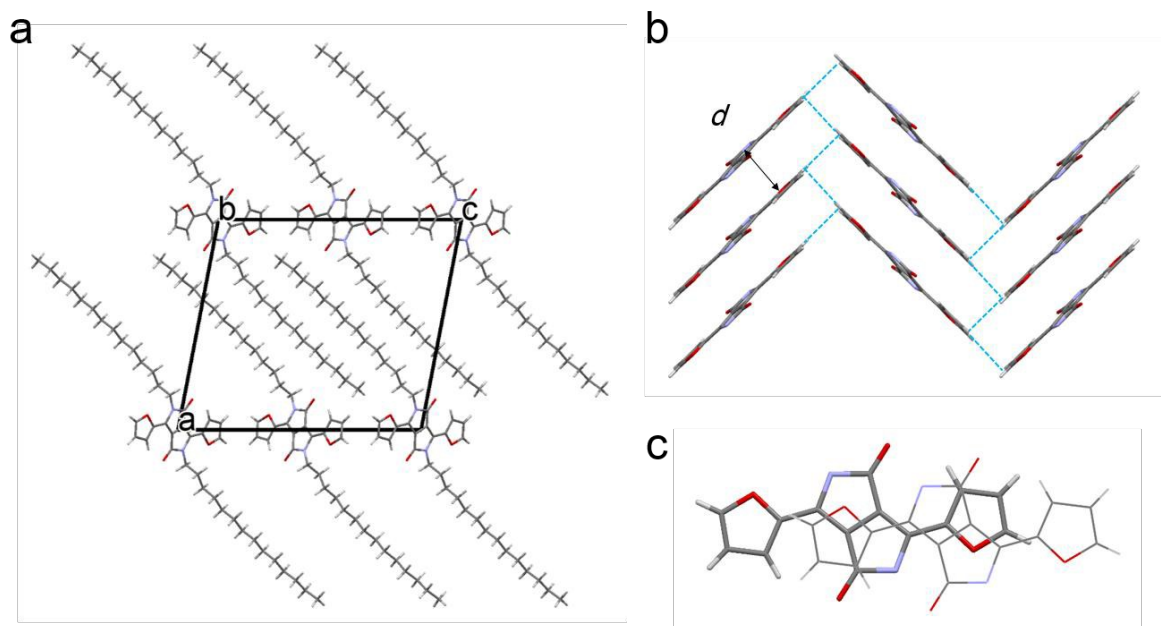
Fig. 2 Single crystal structure of DFDPP-C14 viewed along (a) *b* axis and (b) *a* axis; (c) an overlap in DFDPP-C14 π-stack; blue dotted lines indicate interstack CH…π contacts; alkyl chains are omitted on (b) and (c) for clarity.
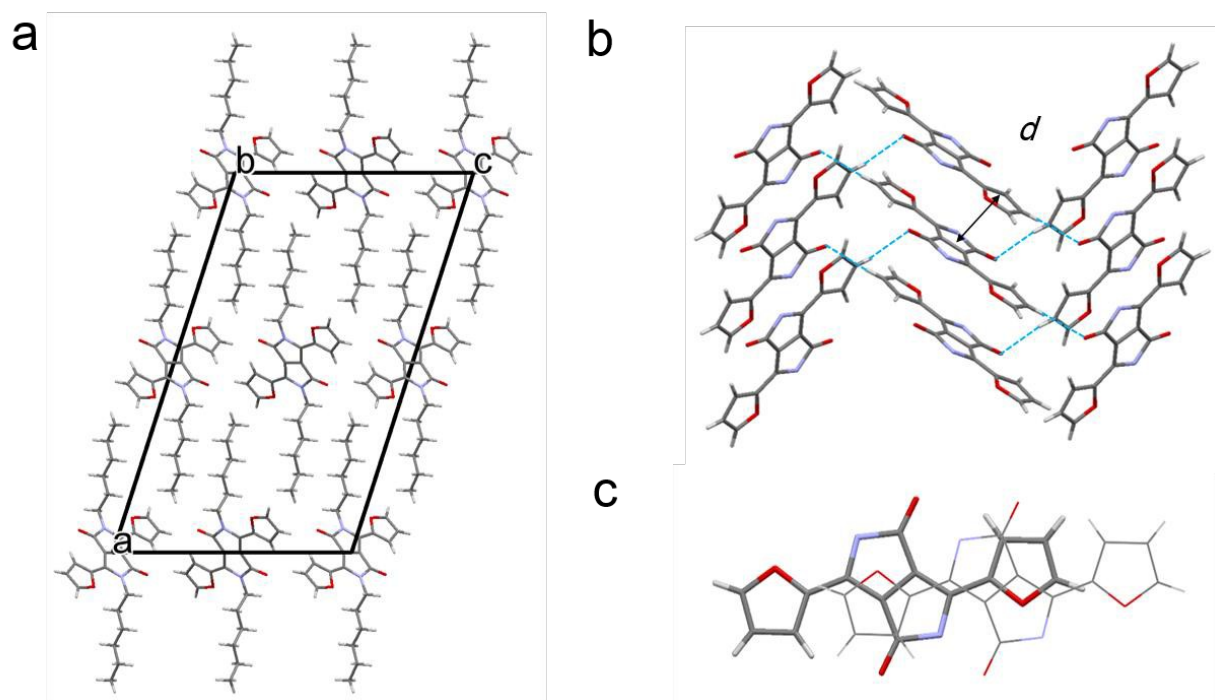
Fig. 3 Single crystal structure of DFDPP-C6 viewed along (a) *b* axis and (b) *a* axis; (c) an overlap in DFDPP-C6 π-stack; blue dotted lines indicate interstack H bonding; hexyl chains are omitted on (b) and (c) for a clarity.

In all cases, spatial accommodation of alkyl chains protruding on both sides of aromatic plane leads to a significant shift in the stacks limiting the degree of π-overlap (Fig. 2 and 3). On the other hand, co-planarization of these chains ($\phi 2=0$) with the DPP core is disfavoured by ca. 5 kcal mol^{-1} (Fig. 1b). While solid state packing and on-surface absorption (see below) forces could potentially overcome this steric strain, coplanarization of the alkyl chain leads an

COMMUNICATION

increasing interring twist for DPDPP (ϕ1=43) whereas DFDPP and DTDPP remain planar.

Molecular self-assembly at the interface is of paramount importance for organic semiconductor devices, as charge transport mainly occurs in the first few layers at the interfaces with metallic electrodes or dielectric substrates buried in device architecture.[23] STM is well suited for such studies, as it provides a submolecular resolutions of the self-assembled monolayers on conducting surfaces. Ordered monolayers of bi-/terthiophene-[24] and phenyl-[25] substituted DPP have been explored by STM earlier showing a face-on adsorption on HOPG. Drop-casting DFDPP-C_{14} solution in tetradecane (ca. 5×10^{-5} M) on highly oriented pyrolytic graphite (HOPG) and annealing at 60°C for 5 min results in formation of similarly ordered monolayer (Fig. 4a). DFDPP-C_{14} self-assembles into alternating dark and bright lamellae with an oblique unit cell (a = 2.6 ± 0.1 nm, b = 1.1 ± 0.1 nm, α = 78 ± 2°). The bright stripes are attributed to the DFDPP π-conjugated cores which possess higher electron density states comparing to the aliphatic chains, which interdigitate forming the dark areas. Within the bright lamellae DFDPP core are resolved as a bright rod, which tilts with respect to the lamella (Fig. 4a inset). Modelling the observed STM structures suggests an antiparallel alignment of the furan moieties of adjacent molecules (Fig. 4b). The resulting weak H-bonding between furan' α-CH and O, as well as van der Waals contacts of the interdigitated alkyl chains appear the key intermolecular interactions driving observed assembly. This proposed molecular model gives a closely matched unit cell: a = 2.6 nm, b = 1.2 nm and α = 77°.

Self-assembly of DFDPP-C_6 under the same conditions leads to a very different, hexagonally packed, structures with not alternating contrast (a = 1.1 ± 0.1 nm, b = 1.2 ± 0.1 nm, α = 60 ± 2°) (Fig. 4c). DFDPP aromatic moieties appear as bright spots similar to the DFDPP-C_{14} but the separation between these spots is insufficient to accommodate alkyl chains. Thus, the hexyl chains are deduced to be desorbed from the HOPG surface, and the corresponding molecular model yields a similar unit cell: a = 1.1 ± 0.1 nm, b = 1.2 ± 0.1 nm and α = 60 ± 2° (Fig. 4d).
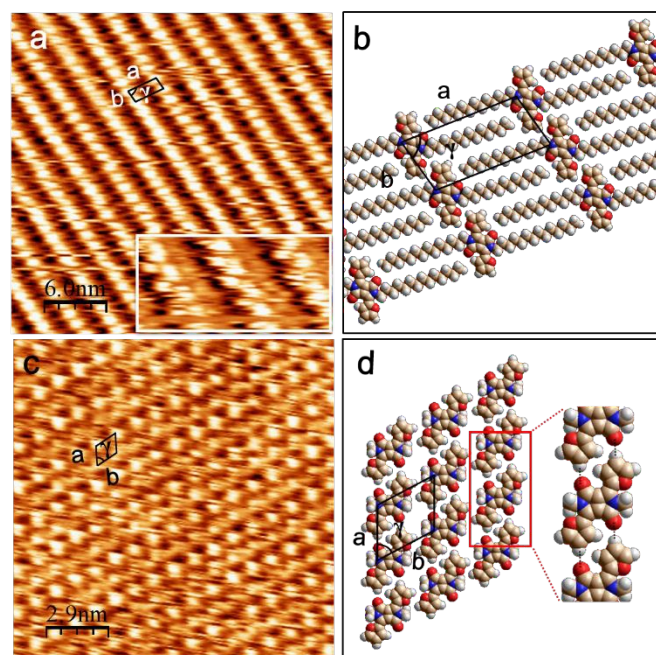
Fig. 4 Self-assembly of DFDPP-Cn (5×10-5 M) at the tetradecane/HOPG interface. (a) STM image of DFDPP-C14 (Vb= 600 mV; It = 0.3 nA). The inset (10.2 nm × 7.3 nm) shows the submolecular features of bright lamellae, and (b) the proposed molecular model. (c) STM image of DFDPP-C6 (Vb= 550 mV; It = 0.3 nA), and (d) the proposed molecular model. The black dotted lines on the enlarged part indicate intermolecular short contacts.

Thus, the alkyl chain length, which causes only minor changes in the 3D supramolecular packing, has a profound effect on the surface self-assembly. A similar behaviour, caused by alkyl chain dewetting from the HOPG substrate, was earlier observed in surface-absorbed monolayers of dialkyl-substituted naphthalenediimide (NDI) semiconductors, which was attributed to a "self-avoiding walk" of alkyl chains in entropy terms.[26] Besides the entropy contribution, our recent study on mono-alkylated NDIs shows the release of intermolecular strain in the out of plain conformation of alkyl chains as the main driving force for this process.[27] In the present case, M06-2X/6-31G(d) calculations (Fig. 1b) show a steric repulsion (2 × 5.5 kcal mol^{-1}) between the DPP oxygens and the β-CH_2 of the alkyl chains when the latter remain in plane with DFPPP, as in fully adsorbed molecules. The adsorption energy gain (~1.3 kcal mol^{-1} per CH_2 [28]) from placing two alkyl chains of DFPDPP-C6 on the surface (~13 kcal mol^{-1}) is only marginally larger than the steric penalty, insufficient to counterbalance the unfavored entropy of this structure. However, the corresponding enthalpic gain for planar adsorption of DFDPP-C_{14} (34 kcal mol^{-1}) clearly predicts a planar orientation of these molecules on the surface.

In conclusion, we have explored the supramolecular assembly of difuryl-DPP molecules in 3D crystals and in surface-adsorbed monolayers. XRD analyses in conjunction with DFT calculations show that the furyl-substituted DPP possess a more planar conjugated backbone and tighter π-π interactions, as compared to other (hetero)aromatic derivatives, suggesting a possibility for more efficient charge

COMMUNICATION

transport. While in bulk solid and gas phase, the alkyl chains on DPP are oriented orthogonally to the conjugated core (which affects the degree of π-overlap), our STM studies show that in surface-adsorbed monolayers the molecules with longer chains tend to fully planarize. We speculate that similar planarization could also be observed in thin films, thus explaining the reported effects that alkyl chains impose on semiconducting properties of DPP-based polymers. [29,16] Considering the enormous popularity of DPP building block, these findings provide a useful insight into the molecular design of semiconducting materials thereof.

Notes and references

‡ Crystallographic and general data for DFDPP-C$_{14}$ (C$_{42}$H$_{64}$N$_2$O$_4$,CCDC 1440141): monoclinic, space group P2$_1$/c, a = 18.8248(10) Å, b = 4.6921(3) Å, c = 21.4035(11) Å, β = 100.903(3)°, V = 1856.40(18) Å^3, Z = 2, T = 105 K, μ(GaKα) = 0.373 mm^{-1}, Dcalc = 1.182 g/cm^3, 30967 reflections measured (7.318° ≤ 2Θ ≤ 121.188°), 4222 unique (Rint = 0.0669, Rsigma = 0.0473) which were used in all calculations. The final R$_1$ was 0.0446 (I > 2σ(I)) and wR$_2$ was 0.1234 (all data). DFDPP-C$_{14}$ (C$_{26}$H$_{32}$N$_2$O$_4$, CCDC 1440140): monoclinic, space group C2/c, a = 28.9402(9) Å, b = 4.8707(2) Å, c = 17.3118(6) Å, β = 107.785(2)°, V = 2323.63(15) Å^3, Z = 4, T = 105 K, μ(GaKα) = 0.434 mm^{-1}, Dcalc = 1.248 g/cm^3, 22074 reflections measured (5.58° ≤ 2Θ ≤ 121.414°), 2663 unique (Rint = 0.0535, Rsigma = 0.0245) which were used in all calculations. The final R$_1$ was 0.0528 (I > 2σ(I)) and wR$_2$ was 0.1521 (all data).

1 A. Iqbal, L. Cassar, A. C. Rochat, J. Pfenninger and O. Wallquist, *J. Coat. Tech.* 1988, **60**, 37.
2 A. B. Tamayo, B. Walker and T.-Q. Nguyen, *J. Phys. Chem. C* 2008, **112**, 11545.
3 Z. Yi, S. Wang and Y. Liu, *Adv. Mater.* 2015, **27**, 3589.
4 Y. Wu and W. Zhu, *Chem. Soc. Rev.* 2013, **42**, 2039.
5 S. Arumugam, R. E. Brown, C. Orofino-Pena, N. J. Findlay, A. R. Inigo, A. L. Kanibolotsky and P. J. Skabara, *Isr. J. Chem*. 2014, **54**, 828.
6 C. B. Nielsen, M. Turbiez and I. McCulloch, *Adv. Mater*. 2013, **25**, 1859.
7 Y. Li, P. Sonar, L. Murphy and W. Hong, *Energy Environ. Sci*. 2013, **6**, 1684.
8 O. Gidron and M. Bendikov, *Angew. Chem. Int. Ed.* 2014, **53**, 2546.
9 O. Gidron, A. Dadvand, Y. Sheynin, M. Bendikov and D. F. Perepichka, *Chem. Commun.* 2011, **47**, 1976.
10 O. Gidron, A. Dadvand, E. W.-H. Sun, I. Chung, L. J. W. Shimon, M. Bendikov and D. F. Perepichka, *J. Mater. Chem. C* 2013, **1**, 4358.
11 C. H. Woo, P. M. Beaujuge, T. W. Holcombe, O. P. Lee and J. M. J. Fréchet, *J. Am. Chem. Soc.* 2010, **132**, 15547.
12 Y. Li, P. Sonar, S. P. Singh, W. Zeng and M. S. Soh, *J. Mater. Chem.* 2011, **21**, 1082.
13 J. C. Bijleveld, B. P. Karsten , S. G. J. Mathijssen , M. M. Wienk, D. M. de Leeuw and R. A. J. Janssen, *J. Mater. Chem.* 2011, **21**, 1600.
14 P. Sonar, T. R. B. Foong, S. P. Singh, Y. Li and A. Dodabalapur, *Chem. Commun.* 2012, **48**, 8383.
15 P. Sonar, S. P. Singh , E. L. Williams , Y. Li , M. S. Soh and A. Dodabalapur, *J. Mater. Chem.* 2012, **22**, 4425.
16 A. T. Yiu, P. M. Beaujuge, O. P. Lee, C. H. Woo, M. F. Toney and J. M. J. Fréchet, *J. Am. Chem. Soc.* 2012, **134**, 2180.
17 M. S. Chen, O. P. Lee, J. R. Niskala, A. T. Yiu, C. J. Tassone, K. Schmidt, P. M. Beaujuge, S. S. Onishi, M. F. Toney, A. Zettl and J. M. J. Fréchet, *J. Am. Chem. Soc.* 2013, **135**, 19229.
18 Y. Li, H. Li, H. Chen, Y. Wan, N. Li, Q. Xu, J. He, D. Chen, L. Wang and J. Lu, *Adv. Funct. Mater.* 2015, **25**, 4246.
19 M.A. Naik, N. Venkatramaiah, C. Kanimozhi and S. Patil, *J. Phys. Chem. C* 2012, **116**, 26128.
20 R. Sevincek, S. Celik, M. Aygun, S. Alp and S. Isik, *Acta Crystallogr. Sect. E.-Struct Rep. Online* 2010, **66**, o1546.
21 J.-D. Huang, S.-H. Wen, W.-Q. Deng and K.-L. Han, *J. Phys. Chem. B,* 2011, **115**, 2140
22 T. Izawa, E. Miyazaki and K. Takimiya, *Adv. Mater.* 2008, **20**, 3388.
23 A. Dodabalapur, L. Torsi and H.E. Katz, *Science* 1995, **268**, 270.
24 T. Jaroch, A. Maranda-Niedbała, M. Góra , J. Mieczkowski, M. Zagórska, M. Salamonczyk, E. Górecka and R. Nowakowski, *Synt. Met.* 2015, **204**, 133.
25 A. Honda, Y. Tamaki and K. Miyamura, *Bull. Chem. Soc. Jpn.* 2015, **88**, 969.
26 Y. Miyake, T. Nagata, H. Tanaka, M. Yamazaki, M. Ohta, R. Kokawa and T. Ogawa, *ACS Nano* 2012, **5**, 3876.
27 C. Fu, H.-P. Lin, J.M. Macleod, A. Krayev, F. Rosei and D.F. Perepichka, *Chem. Mater.* 2016, **28**,951.
28 J. H. Clint, *J. Chem. Soc., Faraday Trans. 1* 1972, **68**, 2239.
29 H. Chen , Y. Guo , Y. Yu , Y. Zhao , J. Zhang , D. Gao , H. Liu and Y. Liu , *Adv. Mater.* 2012, **24**, 4618.

CrystEngComm Accepted Manuscript

A combined XRD, STM and DFT studies reveal the details of supramolecular ordering of difuryldiketopyrrolopyrrole, in monolayers and 3D crystals.